A Versatile PAPR Reduction Algorithm for 5G Waveforms with Guaranteed Performance

Saeed Afrasiabi-Gorgani, Gerhard Wunder
Heisenberg Communications and Information Theory Group
Freie Universität Berlin
s.afrasiabi@fu-berlin.de, wunder@zedat.fu-berlin.de

***Abstract*—Peak-to-Average Power Ratio is a known issue of multicarrier waveforms. As the research on waveform design beyond OFDM is boosted, the PAPR problem has regained attention as a major bottleneck, particularly in spatial multiplexing schemes. In this paper a high-performance and flexible algorithm is proposed inspired by concentration of measure concept. The algorithm is analytically tractable thanks to concentration inequalities as a key element in this work. The performance is guaranteed with rather sharp bounds in a novel way. The PAPR reduction performance of the method for FBMC-OQAM signal model has no degradation comparing to OFDM.**

***Index Terms*—Peak-to-Average Power Ratio (PAPR), Filter Bank MultiCarrier (FBMC), Multiple-Input-Multiple-Output (MIMO), Spatial Multiplexing, concentration inequalities**

I. Introduction

The PAPR problem refers to frequent occurrence of peaks in instantaneous power of the transmit signal that are considerably higher than the average power. The PAPR problem reduces power efficiency in transmitter as nonlinear distortion needs to be controlled by back-off in power amplifier. This problem is particularly a major technological bottleneck in uplink, i.e. handheld devices, due to limited battery life. As the research on waveforms in context of 5G [1] is actively pursued, the PAPR problem has regained attention.

There is considerable research done on this issue. A complete overview and categorization of the proposed solutions needs a separate treatment. The reader is referred to the overview papers in the literature, particularly [2] provides a fundamental viewpoint to the problem. A major category of PAPR reduction methods is based on invertible modifications to the signal. That is, the receiver is able to recover the original data with no distortion due to the PAPR reduction, given that it is aware of the modifications. A classic and well-known method is referred to as Selected Mapping (SLM) [3] which is based on generating several versions of the original complex data sequence for an OFDM symbol by phase rotation of each data symbol. The branch with the lowest PAPR is transmitted. The phase rotations, referred to as side information (SI), are fed-forward to the receiver.

The idea of SLM is based on the fact that the high PAPR is caused by constructive addition of complex exponentials with random amplitude and phase drawn from the specific set of constellation points. If the phase rotations behave statistically "different", the alternative versions of an OFDM symbol with initially high PAPR could have randomly different PAPRs. Consequently, there is a chance that one of the alternatives has a lower PAPR. Clearly, the more alternatives generated, the higher the chance of having a considerably low PAPR. The same principle has been used in many algorithms. If the phase rotations are limited to sign changes ± 1 and a non-random way of choosing them is adopted, we have a class of algorithms referred to as sign selection, sign adjustment, etc.

The PAPR reduction methods can be seen in a different categorization: methods with a focus on low complexity relative to technology of the time and methods with a focus on high performance at the cost of high complexity. The methods belonging to the former category might be moderated versions, hence weaker in performance, of methods from the latter category. The method proposed in this work is focused on sign selection, though extendible, and is a high complexity method.

The algorithm proposed in this work provides PAPR reduction by choosing signs of complex data symbols sequentially. By each sign decision, the goal is to reduce the expected value of the PAPR random variable conditioned on the already fixed signs and fixed data symbols. A sign selection approach has been previously proposed [4], in which limited information is extracted from the search space by essentially fixing all the undecided sign variables to 0. In other words, sign decision is made without considering contribution of data symbols with undecided signs. In contrast, the proposed method exploits the available information by considering expected values. As further explained in the following, the method allows for a performance analysis which provides substantially better upper bounds on reduction, in contrast to the deterministic worst-case bound presented in [4] and similar works.

The process can be described by considering the probability measure of PAPR, which is concentrated around its expected value [2]. Each step of the algorithm shifts the probability measure of the resulting PAPR to left, which has less randomness due to fixed signs. By the last step, the PAPR is no more random and is equal to the last expected value.

PAPR reduction methods are usually first proposed for OFDM signal model. In the recent years, as more advanced waveforms are being considered, there has been attempts to extend the available methods to the new waveforms. One of the pioneering and well-studied waveforms is FBMC with offset QAM, which is also referred to as OFDM/OQAM. A key property of FBMC, and similar waveforms, is that better frequency localization is gained by relaxing the pulse shape from a rectangular pulse in OFDM to pulses spread over more than one symbol interval and smooth. This feature incurs complicity to transceiver algorithms, as the segments of the signal carrying distinct blocks of complex data symbols are no more separated. Particularly, in distortionless PAPR reduction methods, overlapping of adjacent components of the signal raises the problem of handling this interdependency of signal modification on PAPR of the past and future segments of the signal.

Applicability of multi-antenna schemes to a waveform is also an essential area for investigation. There has been a number of works, for instance [5], [6], on spatial multiplexing and diversity schemes using FBMC signal model, which is considerably more challenging that that of OFDM. Considering that research on MIMO FBMC does not seem to have converged to a standard way, we focus only on spatial multiplexing with independent data streams on antennas. We also make a simplifying assumption that all the required processing is done in the receiver, i.e. no modification to the signal model is done to accommodate the detection in the receiver.

The rest of the paper is organized as follows: Section II formally described the PAPR problem. Then the signal model of interest is explained in Section III. The proposed algorithm with the provided analysis are developed in Sections IV and V. Finally, the PAPR reduction performance is investigated by simulations in Section VI.

II. The PAPR problem

In order to characterize time domain fluctuation of the signal from the power amplifier's point of view, PAPR is measured over short intervals. In addition, oversampling by a factor of L is necessary to detect the peaks accurately. For OFDM, time-domain isolation of signal segments that are constructed from different blocks of N data symbols gives a natural interval duration of LN samples for PAPR measurement. However, any length is valid. For FBMC signal no such isolation exists between consecutive components. For comparison purposes, we keep the same LN samples for measurement of PAPR for FBMC signal. Note that the power amplifier input is the passband signal. The PAPR reduction algorithms, however, operate in digital baseband part of the transmitter. As a common metric, the PAPR of baseband signal is considered.

Such characterization gives a random variable defined for the i^{th} antenna as

$$\gamma^{(i)} = \frac{\max_{n\in\{0,1,\ldots,LN-1\}} |s(n)|^2}{P_a}, \tag{1}$$

where $P_a = \mathrm{E}[|s(n)|^2]$ is the average power and it is assumed that the interval of interest is shifted to begin at $n = 0$ for simplicity.

The PAPR problem exhibits itself as a more challenging problem when multiple antennas are used in the transmitter. The distortion caused by high PAPR of multicarrier signals causes two problems: in-band distortion and out-of-band distortion. In multiple transmit antennas, the worst level of out-of-band radiation dominates. In other words, the PAPR problem of N_t antennas transmitting independent data streams in parallel can be characterized by the worst PAPR in each signaling interval. In spatial multiplexing, this is equivalent to measuring PAPR of a single antenna transmitter over N_t times longer duration. Formally,

$$\gamma = \max_{i\in\{1,2,\ldots,N_t\}} \gamma^{(i)} \tag{2}$$

Notice that in OFDM, γ is simply a function of a single block of N data symbols on which the PAPR is measured. In FBMC, on the other hand, it is a function of several consecutive N-blocks. This dependence is further investigated by considering the FBMC signal model.

It is common to use the complementary cumulative distribution function (CCDF) to interpret the behavior of γ. A sample reading from such a curve might be as follows: The PAPR of OFDM or FBMC signal for $N = 1024$ subcarriers exceeds 11.7 dB with a probability of 10^{-3}. Further implications of this reading on performance of the system depends on a number of other factors and an accurate discussion is beyond the scope of this work. To facilitate the discussions, the constant *effective PAPR* γ_ϵ is defined such that

$$\mathbb{P}(\gamma > \gamma_\epsilon) = \epsilon, \tag{3}$$

where ϵ is taken as 10^{-3} for reporting PAPR reduction in this work.

III. Signal model

One of the most studied waveforms to replace OFDM is FBMC with offset QAM. A very brief description is that FBMC allows for better designed pulse shapes by working with purely real data symbols, but with a spectral efficiency of 2. Therefore, QAM symbols are broken into two pieces together with some other modifications necessary for the orthogonality, which constitutes what is referred to as offset QAM (OQAM). Desirable localization of pulses in frequency domain dictates some spreading in time-domain, which leads to overlapping among the waveform components pertaining to subsequent blocks of N data symbols. In the following description, an OFDM or FBMC symbol refer to the waveform component based on a block of N complex data symbols, or a segment of the signal associated with that block.

In the signal model presented in the following, oversampling is included which is essential for PAPR measurement which is in turn often required in iterative PAPR reduction algorithms. The FBMC signal transmitted from i^{th} antenna is [7]

$$s^{(i)}(n) = \sum_{m=-\infty}^{+\infty} \sum_{k=0}^{N-1} (a_{n,2m}\gamma_{n,2m}(p) + a_{n,2m+1}\gamma_{n,2m+1}(p)). \tag{4}$$

where

$$\gamma_{k,q}(n) = h^L[n - qL\frac{N}{2}] e^{j\frac{2\pi}{LN}k(n-\frac{L_h-1}{2})} e^{j\phi_{k,q}}. \tag{5}$$

The parameter L_h denotes the pulse filter length. In addition, $h^L(n)$ is the oversampled discrete-time pulse. Notice that the

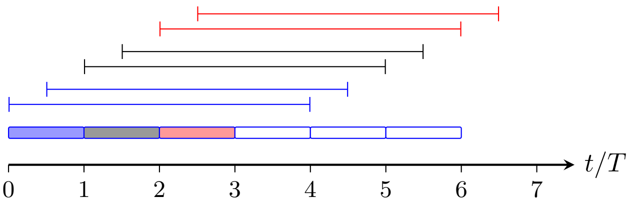

Fig. 1. Illustration of FBMC symbols for $K = 4$. Plain lines show the subsymbols, each pair of which belongs to one FBMC symbol. A rectangle shows the overall signal in one FBMC signaling interval, constructed by adding the subsymbols in the same interval.

signaling interval T for FBMC symbols is equivalent to LN samples. $a^{(i)}_{2m,k}$ and $a^{(i)}_{2m+1,k}$ are purely real processed symbols taken from complex QAM data symbols which belong to antenna i, block m and subcarrier k.

Note that $h(n)$ is causal and truncated to the interval $n \in \{0, 1, \ldots, KN-1\}$. The signaling interval is the distance between insertion point of two consecutive waveform components related to two consecutive blocks of N data symbols, which is LN samples. These should justify the length of the waveform component for an N-block of data symbols to be equal to $(K+1/2)LN$. Specifically, the signal on each antenna can be written as

$$s(n) = \sum_{m=-\infty}^{+\infty} s_m(n) \tag{6}$$

where antenna index i is dropped and

$$s_m(n) = \sum_{k=0}^{N-1} (a_{k,2m}\gamma_{k,2m}(n) + a_{k,2m+1}\gamma_{n,2m+1}(n)). \tag{7}$$

The overlapping of symbols is depicted in Fig. 1. In order to formulate the overlapping of neighboring symbols, (6) is written as

$$\begin{aligned} s(n) &= \sum_{m=-\infty}^{m_0-1} s_m(n) + s_{m_0}(n) + \sum_{m=m_0+1}^{+\infty} s_m(n) \\ &= p(n) + s_{m_0}(n) + t(n), \end{aligned} \tag{8}$$

with $s_{m_0}(n)$ being the collection of terms over which PAPR reduction is to be performed. The terms modulated by the past and future data symbols are gathered in $p(n)$ and $t(n)$, respectively. Let the time index $n = 0$ indicate the first nonzero sample of $s_{m_0}(n)$. Then the first nonzero sample of $t(n)$ occurs at $n = LN$.

A desired algorithm should minimize the PAPR of the samples in $s_{m_0}(n)$ by taking into account the overlapping part of $p(n)$. The samples from $t(n)$ are clearly not available yet. After processing the m_0^{th} FBMC symbol, the samples of $p(n) + s_{m_0}(n)$ for $n \in \{0, 1, \ldots, LN-1\}$ are ready for transmission and the remaining $((K-1) + \frac{1}{2})LN$ samples must be *buffered* for the next symbol(s).

IV. Proposed Method

Let $\mathbf{C}$ be a random vector of complex data symbols and $\mathbf{X}$ be the corresponding vector of sign changes. Consider a cost function

$$f(\mathbf{C}, \mathbf{X}) = \max_n |p(n) + s_{m_0}(n)|, \tag{9}$$

following the definitions in (8) such that data symbols are replaced by $[C_0X_0, C_1X_1, \ldots, C_{N-1}X_{N-1}]^T$, i.e. element-wise multiplication of data symbols and sign variables.

The objective is to reduce PAPR by making a decision on sign variable x_j such that [8]

$$\mathrm{E}[f(\mathbf{C}, \mathbf{X})|\mathbf{c}, x^*_{0:j}] = \min_{x_j \in \{-1,1\}} \mathrm{E}[f(\mathbf{C}, \mathbf{X})|\mathbf{c}, x^*_{0:j-1}, x_j] \tag{10}$$

It can be shown that such decisions on sign variables result in the sequence of conditional expectations

$$\begin{aligned} z_0 &= \mathrm{E}_{X_{0:N-1}}[f(\mathbf{X}, \mathbf{C})|\mathbf{c}] \\ &\vdots \\ z_j &= \mathrm{E}_{X_{j:N-1}}[f(\mathbf{X}, \mathbf{C})|x^*_{0:j-1}, \mathbf{c}] \\ &\vdots \\ z_n &= \mathrm{E}_{\emptyset}[f(\mathbf{X}, \mathbf{C})|\mathbf{x}^*, \mathbf{c}] = f(\mathbf{x}^*, \mathbf{c}). \end{aligned} \tag{11}$$

Further more, we have [8]

$$z_0 \geq z_1 \geq \ldots \geq z_n. \tag{12}$$

That is, the last conditional expectation is over a constant variable and yields the PAPR value $f(\mathbf{x}^*, \mathbf{c})$. In addition, it is upper-bounded by initial one. Therefore, the sign decision rule of (10) leads to PAPR reduction in a tractable way.

Furthermore, (12) implies that for any subset of sign variables the same trend holds. It is reported [8] that first sign variables, i.e. those with lower indices, have relatively low impact on the PAPR reduction. Therefore, a *refined algorithm* is proposed that uses a subset of sign variables with indices ending at $N-1$.

A. Calculation of conditional expectations

Clearly, calculation of conditional expectations is a key element of the algorithm. In particular, with PAPR as the choice for f, analytic calculation of the conditional expectations is not available and estimation is used as an intermediate solution. Let $\mathbf{c} \in \mathcal{M}^n$ be realization of the random vector of complex data symbols. For making decision on the j^{th} sign variable, we need to obtain

$$g^{\pm}_j(\mathbf{c}) = \mathrm{E}[f(\mathbf{C}, \mathbf{X})|\mathbf{C} = \mathbf{b}, X_{0:j-1} = x^*_{0:j-1}, X_j = \pm 1], \tag{13}$$

the estimated value of which is obtained by a sample average with Q shots:

$$\hat{g}^{\pm}_j(\mathbf{c}) = \frac{1}{Q}\sum_{l=1}^{Q} f(\mathbf{C}, \mathbf{X}^l)|_{\mathbf{C}=\mathbf{c}, X^l_{0:j-1}=x^*_{0:j-1}, X^l_j=\pm 1}, \tag{14}$$

where $\mathbf{X}^l$ has the same distribution as $\mathbf{X}$. Clearly $\mathrm{E}[\hat{g}_j(\mathbf{c})] = g_j(\mathbf{c})$.

It will be shown in Section V that it is possible to approach distribution of the estimation via concentration inequalities.

B. Side Information

An important aspect of such distortionless PAPR reduction methods is undoing the modifications in the receiver. The possible options include

- A reliable transmission of the required information.
- Using implicit side information.
- Discarding the signs of data symbols in receiver.

The first option, i.e. feed-forwarding of the modifications to the receiver, is related to availability of such channel and needs to be embedded in a protocol. Therefore, its feasibility depends on many other factors. The second option is a different, but related, algorithmic challenge. The third option can be viewed as a coding that adds a single (sign) bit to each complex data symbol on a set of subcarriers. This bit is discarded in the receiver.

As a conclusion, we suffice to reporting the rate loss incurred by the third option. Note that this causes the same rate loss as the amount of SI required for undoing the process when all or a pre-determined subset of data symbols undergo a separate modification. The rate loss due to the refined algorithm on signs variables $x_{v:N-1}$ is

$$r_l(v) = \log_2 |\mathcal{M}| - \frac{1}{N} \log_2 \left[|\mathcal{M}|^v \left(\frac{|\mathcal{M}|}{2} \right)^{N-v} \right] = \frac{N-v}{N}. \quad (15)$$

Therefore, for the case of $v = n/2$, the rate loss is 0.5 b/sym instead of 1 b/sym for 16QAM modulation. Clearly, for a constellation of higher size the rate loss decreases.

C. MIMO extension

In this work, spatial multiplexing with N_t independent streams of data symbol on each antenna is assumed. That is, the waveforms on different antennas are not coupled in anyway. As explained before, the worst PAPR needs to be minimized over each measurement interval. Therefore, either a cost function f dependent on all streams must be defined or a strategy must be adopted to apply the same cost function to different branches. A trivial approach is to identically perform the reduction method on each antenna. It is interesting to see if a better performance can be achieved at the same complexity and rate loss.

A very successful yet simple idea is directed SLM (dSLM) [9] which takes generation of each alternative signal by a new phase vector, as done in SLM method, as a resource unit. Instead of allocating equal number of resource units to every antenna, they are allocated step by step to the antenna with the worst PAPR at each iteration. That is, if there are U total phase vectors available, ordinary SLM (oSLM) would do SLM on each antenna with U/N_t branches, while dSLM makes no

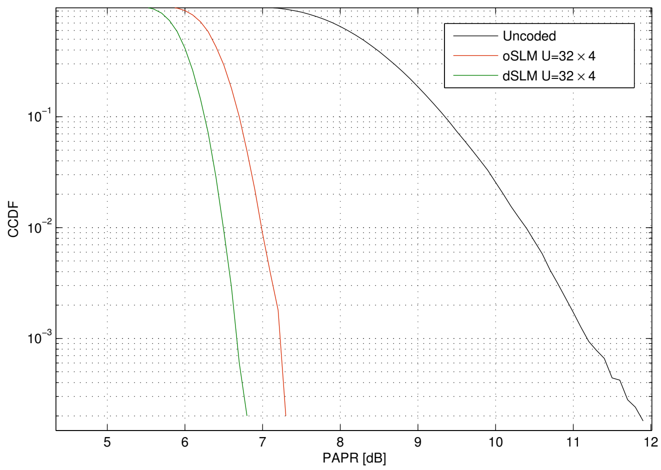

Fig. 2. Performance of dSLM versus oSLM showing how mimization of worst-case PAPR of several independent branches allows better results. $N = 64$, 16QAM, $N_t = 4$, U=128. That is, 32 phase vectors per branch for oSLM and $32 \times 4 = 128$ phase vectors for dSLM.

prediction for the number of resource units required for each branch. It turns out that dSLM performs considerably better than oSLM for the same amount of computational resources, which indicates that minimization of worst-case PAPR offers more freedom.

Fig. 2 shows the performance of dSLM for 64 subcarriers and 16QAM and 4 antennas. Note that a reduction of 4.5 dB is achievable for 32×4 phase vectors, while the corresponding oSLM with 32 phase vectors per antenna provides about 4 dB of reduction.

Concerning the proposed method for sign selection, a dynamic resource allocation targeting the worst PAPR is interesting. In this scheme each sign variable, hence sign decision, is considered as a resource unit. Note that sign decision at each iteration is done by comparing conditional expectations over the remaining undecided sign variables. This leads to a decreasing trajectory of conditional expectations which at the last step coincides with the reduced PAPR value. Therefore, a change in number of sign variables once the formation of trajectory is started causes disruption in the working of the algorithm. In other words, a key fact about the algorithm is that the number of sign variables for each branch must remain unchanged during the process for each symbol interval.

A strategy to keep the rate saving of refined algorithm by using an ending subset of signs is as follows. For each symbol, resource units are assigned according to the initial PAPR values, constrained by a minimum and maximum number, such that the branch with the lowest PAPR always gets the minimum and the branch with the largest always gets the maximum. Formally, consider γ_k represent initial PAPR of the k^{th} branch. The minimum number of signs per branch is denoted by $\rho_{\min}$ and the maximum by $\rho_{\max}$. The number of assigned signs for branch k is given by the mapping

$$\rho_k = \left(\frac{1}{1-\gamma_{\min}} \frac{\gamma_k}{\gamma_{\max}} - \frac{\gamma_{\min}}{1-\gamma_{\min}} \right) (\rho_{\max} - \rho_{\min}) + \rho_{\min}. \quad (16)$$

Then sign variables active for branch k have indices $N-\rho_k : N-1$. The performance of this strategy is discussed in Section VI.

V. Analysis

Two aspects of the algorithm could benefit from some analytic investigation: PAPR reduction capability and estimation of conditional expectations. In both cases, the concentration inequalities prove to be applicable tools while standard ways might be tedious and out of reach.

A. Estimation of Conditional Expectations

Statistical behavior of the estimator in Section V is difficult to analyze due to the maximum operator in definition of PAPR metric. However, it will be shown that using concentration inequalities, probability of deviation of the estimation from its true value can be upper bounded.

Here we use the McDiardmid's inequality. Given that random variables X_i are independent, if it can be shown for $u(\mathbf{X})$ that

$$|u(\mathbf{x})-u(\mathbf{x}')| \le d_k \tag{17}$$

when only the k^{th} component of $\mathbf{x}$ and $\mathbf{x}'$ disagree, McDiarmid's inequality holds and states that for every $\alpha \ge 0$

$$\mathbb{P}(|u(\mathbf{X})-\mathrm{E}[u(\mathbf{X})]| \ge \alpha) \le 2e^{-\frac{2\alpha^2}{\sum_k d_k^2}}. \tag{18}$$

To drive the inequality the bounded differences of (17) must be considered for $\hat{g}_j$. For iteration j, consider $\mathbf{X}^{1:Q}$ and $\mathbf{Y}^{1:Q}$ such that $\mathbf{X}^l \in \{-1,1\}^N$, $\mathbf{Y}^l \in \{-1,1\}^N$. As there are $j-1$ sign decisions already made, $X^l_{0:j-1} = Y^l_{0:j-1} = x^*_{0:j-1}$ for $l = 1,\dots,Q$ are constant. The single disagreement between $\mathbf{X}^{1:Q}$ and $\mathbf{Y}^{1:Q}$ is such that $X^l_m = Y^l_m$ for all l and m except for l' and m'. That is, $X^{l'}_{m'} = -Y^{l'}_{m'}$. Then we have

$$\begin{aligned}
|\hat{g}_j(\mathbf{c},\mathbf{X}^{1:Q}) - \hat{g}_j(\mathbf{c},\mathbf{Y}^{1:Q})| &= \left|\frac{1}{Q}\sum_{l=1}^{Q}\left[f(\mathbf{c},\mathbf{X}^l) - f(\mathbf{c},\mathbf{Y}^l)\right]\right| \\
&= \left|\frac{1}{Q}\sum_{l=1}^{Q}\left[\max_k |s(k,\mathbf{X}^l)| - \max_k |s(k,\mathbf{Y}^l)|\right]\right| \\
&\le \frac{1}{Q}\sum_{l=1}^{Q}\left|\max_k |s(k,\mathbf{X}^l)| - \max_k |s(k,\mathbf{Y}^l)|\right| \\
&\le \frac{1}{Q}\sum_{l=1}^{Q}\max_k \left|s(k,\mathbf{X}^l) - |s(k,\mathbf{Y}^l)\right| \\
&= \frac{1}{Q}\frac{1}{\sqrt{NP_a}}2|c_m| \le \frac{1}{Q}\frac{1}{\sqrt{NP_a}}d
\end{aligned} \tag{19}$$

where

$$|\max|p(t)| - \max|q(t)|| \le \max|p(t)-q(t)| \tag{20}$$

is used and $d = 2\max_{x\in\mathcal{M}}|x|$. Then McDiarmaid's inequality shows that for $\alpha \ge 0$

$$\mathbb{P}(|\hat{g}^{\pm}_j(\mathbf{c}) - g^{\pm}_j(\mathbf{c})| \ge \alpha) \le 2\exp\left(-\alpha^2\frac{2P_a}{d^2}\frac{QN}{(N-j)}\right) \tag{21}$$

This forms a relation between number of shots Q and probability of deviation by α from the true values.

The above analysis on the estimations can be related to sign decision as follows. Without loss of generality, assume that $g^+_j(\mathbf{c}) < g^-_j(\mathbf{c})$ and let $g^*_j(\mathbf{c}) = g^+_j(\mathbf{c})$ denote the lower expectation, i.e. the one belonging to the desired sign. The other case follows from re-labeling. Furthermore, let $\hat{g}^*_j(\mathbf{c}) = \min\{\hat{g}^+_j(\mathbf{c}), \hat{g}^-_j(\mathbf{c})\}$. Here we show that the following bound holds for $\alpha \ge 0$.

$$\mathbb{P}\left(\left|\hat{g}^*_j(\mathbf{c}) - g^*_j(\mathbf{c})\right| \ge \alpha\right) < 4\exp\left(-\alpha^2\frac{2P_a}{d^2_{\max}}\frac{QN}{(N-j)}\right) \tag{22}$$

Assume that $|\hat{g}^{\pm}_j(\mathbf{c}) - g^{\pm}_j(\mathbf{c})| < \alpha$. There are two cases:

1) $\hat{g}^+_j(\mathbf{c}) \le \hat{g}^-_j(\mathbf{c})$: here the estimates follow the true order so that $\hat{g}^*_j(\mathbf{c}) = \hat{g}^+_j(\mathbf{c})$. Hence
$$g^*_j(\mathbf{c}) - \alpha < \hat{g}^*_j(\mathbf{c}) < g^*_j(\mathbf{c}) + \alpha.$$
2) $\hat{g}^+_j(\mathbf{c}) > \hat{g}^-_j(\mathbf{c})$: here the estimates follow NOT the true order so that $\hat{g}^*_j(\mathbf{c}) = \hat{g}^-_j(\mathbf{c})$. We have
$$\hat{g}^-_j(\mathbf{c}) > g^-_j(\mathbf{c}) - \alpha \ge g^+_j(\mathbf{c}) - \alpha = g^*_j(\mathbf{c}) - \alpha$$
and
$$\hat{g}^-_j(\mathbf{c}) < \hat{g}^+_j(\mathbf{c}) < g^+_j(\mathbf{c}) + \alpha = g^*_j(\mathbf{c}) + \alpha.$$

Hence $|\hat{g}^{\pm}_j(\mathbf{c}) - g^{\pm}_j(\mathbf{c})| < \alpha$ implies $|\hat{g}^*_j(\mathbf{c}) - g^*_j(\mathbf{c})| < \alpha$. Therefore,

$$\begin{aligned}
\mathbb{P}\left(\left|\hat{g}^*_j(\mathbf{c}) - g^*_j(\mathbf{c})\right| \ge \alpha\right) \le \mathbb{P}\left(\left|\hat{g}^+_j(\mathbf{c}) - g^+_j(\mathbf{c})\right| \ge \alpha\right) \\
+ \mathbb{P}\left(\left|\hat{g}^-_j(\mathbf{c}) - g^-_j(\mathbf{c})\right| \ge \alpha\right)
\end{aligned} \tag{23}$$

which gives the desired result using (21).

Despite the provided analysis on estimation of conditional expectations, establishing a direct relation to the PAPR reduction performance remains a problem to tackle.

B. Bounds on PAPR reduction

The sequence of conditional expectations in (11) gives z_0 as the upper bound on z_n, which is the reduced value of f. The constant z_0 can be seen as realization of random variable Z_0 which is a function of only $\mathbf{C}$. This can provide two general methods for investigating the performance of the algorithm: a) Analysis of distribution of Z_0 by concentration inequalities, b) numerically estimating the distribution of Z_0.

Concentration of Crest Factor of the OFDM signal around its expected value is studied in [10], [2], [11] using concentration inequalities. In [8] McDiarmid's inequality is applied in a slightly different way to establish concentration of the partial expectation Z_0 around $\mu = \mathrm{E}[f(\mathbf{C},\mathbf{X})]$ to derive

$$\mathbb{P}(\mathrm{E}[f(\mathbf{C},\mathbf{X})|\mathbf{C}] - \mathrm{E}[f(\mathbf{C},\mathbf{X})] \ge \alpha) \le e^{-2\alpha^2 P_a/d^2}. \tag{24}$$

A numerical approach to performance analysis requires offline estimation of distribution of Z_0 [8]. This can be better appreciated by referring to Fig. 3 where the CCDF of Z_0 is used to represent a random upperbound. Unfortunately, the concentration inequalities applied to the problem do not turn out to be very informative. On the other hand, estimated distribution of Z_0 provides a rather *brick-wall* upper-bound.

The estimation approach to reduced PAPR upperbound can be further analyzed as follows. The term $\mathrm{E}[f(\mathbf{X}, \mathbf{C})]$ can be estimated with arbitrary α-deviation for fixed outage probability using q-shot estimator before and again by applying concentration inequalities. The *average reduction capability* under the proposed algorithm is then given by

$$\mathrm{E}[f(\mathbf{X}^{*}, \mathbf{C})\,|\mathbf{C}] \leq \frac{1}{Q}\sum_{l=1}^{Q} \hat{g}_0\left(\mathbf{C}^{l}\right) + N\alpha \tag{25}$$

where the inequality holds with probability given by (21) within α-deviation and $\mathbf{X}^{*}$ is the estimated sign vector in each iteration. The additional n-fold α-deviation stems from the fact that the estimated conditional expectation deviates from the true value by α in each deviation.

VI. Simulation

As discussed before, detection performance, i.e. effects on bit error rate, is irrelevant as the proposed method is a distortionless method. Therefore, only the waveform generation in transmitter is simulated to measure the PAPR. The investigation is thoroughly done for single antenna OFDM model in [8], including comparison with methods of the same class and a few well-known methods in terms of performance and rate loss . Here the proposed algorithm is applied to FBMC signal model, as well as a multiple antenna with independent data streams in OFDM model.

As discussed in [8], the method provides a considerable PAPR reduction even for fairly low number of shots, e.g. $Q = 5$, in estimation of conditional expectations. Focusing on performance versus rate loss, rather than complexity, a higher number of shots $Q = 100$ is used throughout the following simulations. The performance increases slowly for higher Q.

The CCDF curves for the case of single antenna OFDM with $N = 64$, QPSK and 16QAM modulation orders are shown in Fig. 3. The curve labeled “uncoded” refers to the original signal with no PAPR reduction. It can be seen that the algorithm works better for a lower modulation order. This behaviour is shown in the upper bound curves as well. In addition to $Q = 100$, number of subcarriers and modulation order used in the rest of the simulations are fixed to $N = 64$ and 16QAM.

The performance of the algorithm for FBMC signal model as specified in Section IV is shown in Fig. 4. Notice that the performance is nearly identical to that of OFDM despite the overlappings and the expected performance degradation due to lack of control over the already transmitted segments of signal. This observation is reported in [12] too for application of a derandomized PAPR reduction algorithm to the FBMC signal model. It must be mentioned that the uncoded, i.e. original, CCDF curve of OFDM and FBMC signal models are identical.

The extension of the algorithm to multiple antennas with independent data streams is done for OFDM signal model. The simulation result for $N = 64$, 16QAM and $N_t = 4$ is shown

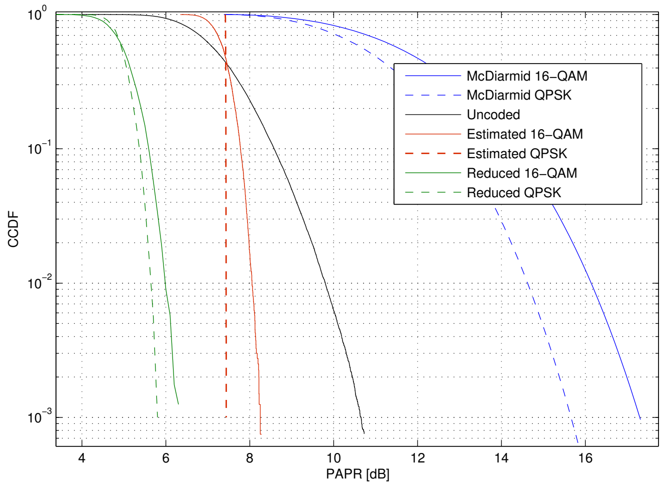

Fig. 3. A representation of the random upper-bound on reduced PAPR by the CCDF curves, for $N = 64$, estimated by generously high Q.

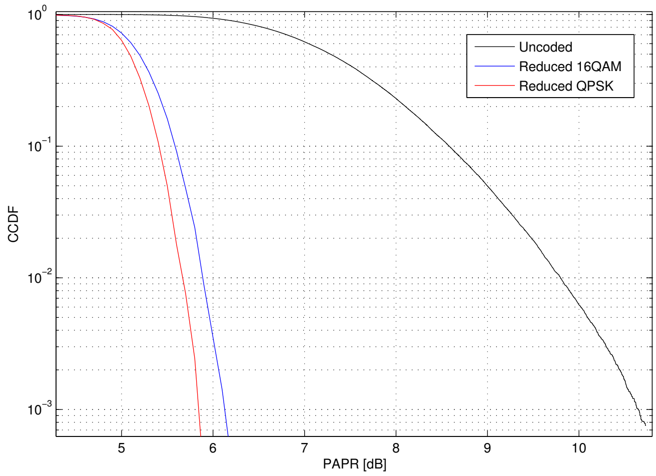

Fig. 4. PAPR reduction performance of the proposed algorithm for FBMC-OQAM signal model and single antenna, for $N = 64$.

in Fig. 5. It can be shown from simulations that the average number of signs per branch for the case of $N = 64$, $\rho_{\min} = N/4$ and $\rho_{\max} = N/2$ is about 22. An ordinary scheme with this number of signs per branch would provide about 3.6 dB reduction in effective PAPR while this strategy yields about 4.2 dB reduction. Clearly, the rate loss in the ordinary case is lower which could make it a more appealing case. However, the strategy is pursued mostly for further investigation of the working of the proposed PAPR reduction method.

VII. Conclusion

A distortionless PAPR reduction algorithm by sign selection which was first proposed in [8] is further investigated in two areas. The method is applied to FBMC signal model, which has overlapping between neighbouring signal components related to consecutive block of data symbols. As the algorithm makes decision on sign of data symbols of a single block, the overlapping part on the future signal segments cannot be

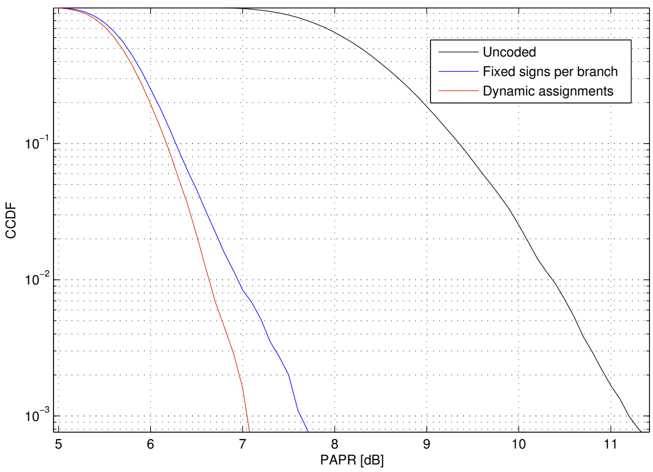

Fig. 5. Dynamic sign assignment versus fixed 22 signs assigned to each branch. for $N = 64$, $\rho_{\min} = N/4$ and $\rho_{\max} = N/2$ which gives an average assigned sign per branch of about 22.

modified. Despite this complicity, it is shown by simulation that the PAPR reduction performance is not degraded. The second area of investigation is MIMO, specifically multiple antennas with independent data streams. A strategy following a similar idea to that of directed SLM (dSLM) [9] is presented and its performance is evaluated. Although the proposed strategy improves the performance, it does not add the remarkable boost that dSLM adds to ordinary SLM.

Acknowledgements

This work was supported by German Research Foundation (DFG) under grant WU 598/3-1.

References

[1] G. Wunder, P. Jung *et al.*, "5GNOW: non-orthogonal, asynchronous waveforms for future mobile applications," *Communications Magazine, IEEE*, vol. 52, no. 2, pp. 97–105, February 2014.

[2] G. Wunder, R. F. H. Fischer, H. Boche, S. Litsyn, and J.-S. No, "The PAPR problem in OFDM transmission: New directions for a long-lasting problem," *The IEEE signal processing magazine*, vol. abs/1212.2865, 2013.

[3] R. Bauml, R. F. H. Fischer, and J. Huber, "Reducing the peak-to-average power ratio of multicarrier modulation by selected mapping," *Electronics Letters*, vol. 32, no. 22, pp. 2056–2057, Oct 1996.

[4] M. Sharif, V. Tarokh, and B. Hassibi, "Peak power reduction of OFDM signals with sign adjustment," *Communications, IEEE Transactions on*, vol. 57, no. 7, pp. 2160–2166, July 2009.

[5] T. Ihalainen, A. Ikhlef, J. Louveaux, and M. Renfors, "Channel Equalization for Multi-Antenna FBMC/OQAM Receivers," *Vehicular Technology, IEEE Transactions on*, vol. 60, no. 5, pp. 2070–2085, Jun 2011.

[6] R. Zakaria and D. Le Ruyet, "Partial ISI cancellation with viterbi detection in MIMO filter-bank multicarrier modulation," in *Wireless Communication Systems (ISWCS), 2011 8th International Symposium on*, Nov 2011, pp. 322–326.

[7] P. Siohan, C. Siclet, and N. Lacaille, "Analysis and design of OFDM/OQAM systems based on filterbank theory," *Signal Processing, IEEE Transactions on*, vol. 50, no. 5, pp. 1170–1183, May 2002.

[8] S. Afrasiabi-Gorgani and G. Wunder, "Multicarrier PAPR reduction by iteratively shifting and concentrating the probability measure," *ArXiv e-prints*, 2015.

[9] R. Fischer and M. Hoch, "Peak-to-Average Power Ratio Reduction in MIMO OFDM," in *Communications, 2007. ICC '07. IEEE International Conference on*, June 2007, pp. 762–767.

[10] I. Sason, "On the concentration of the crest factor for OFDM signals," in *Wireless Communication Systems (ISWCS), 2011 8th International Symposium on*, Nov 2011, pp. 784–788.

[11] S. Litsyn and G. Wunder, "Generalized bounds on the crest-factor distribution of ofdm signals with applications to code design," *Information Theory, IEEE Transactions on*, vol. 52, no. 3, pp. 992–1006, March 2006.

[12] S. Afrasiabi Gorgani and G. Wunder, "Derandomized multi-block sign selection for PMEPR reduction of FBMC waveform," in *Vehicular Technology Conference (VTC Spring), 2015 IEEE 81th*, May 2015.